ACS central science

http://pubs.acs.org/journal/acscii

Outlook

Toward High Performance Anodes for Sodium-Ion Batteries: From Hard Carbons to Anode-Free Systems

Zhaoguo Liu, Ziyang Lu,* Shaohua Guo, Quan-Hong Yang, and Haoshen Zhou*

Cite This: *ACS Cent. Sci.* 2023, 9, 1076−1087

Read Online

ACCESS | Metrics & More | Article Recommendations

ABSTRACT: Sodium-ion batteries (SIBs) have been deemed to be a promising energy storage technology in terms of cost-effectiveness and sustainability. However, the electrodes often operate at potentials beyond their thermodynamic equilibrium, thus requiring the formation of interphases for kinetic stabilization. The interfaces of the anode such as typical hard carbons and sodium metals are particularly unstable because of its much lower chemical potential than the electrolyte. This creates more severe challenges for both anode and cathode interfaces when building anode-free cells to achieve higher energy densities. Manipulating the desolvation process through the nanoconfining strategy has been emphasized as an effective strategy to stabilize the interface and has attracted widespread attention. This Outlook provides a comprehensive understanding about the nanopore-based solvation structure regulation strategy and its role in building practical SIBs and anode-free batteries. Finally, guidelines for the design of better electrolytes and suggestions for constructing stable interphases are proposed from the perspective of desolvation or predesolvation.

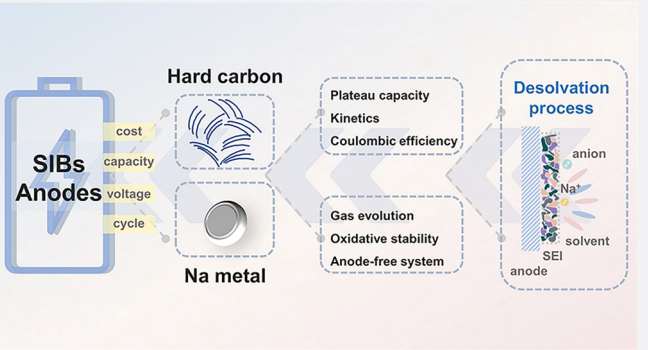

1. INTRODUCTION

Compared with lithium (Li), sodium (Na) is more evenly distributed in the Earth's crust and has much higher reserves, which greatly reduces the cost of sodium-ion batteries (SIBs). Furthermore, the anode of a SIB is compatible with cheap and lightweight aluminum current collectors, which makes SIB technology more sustainable than lithium-ion batteries (LIBs). Therefore, SIBs hold great potential in large-scale energy storage to meet the development of intermittent renewable energy power generation technology.[1] Cathode materials have exhibited appealing electrochemical performance and acceptable cost, including sodium transitional metal oxides, Prussian blue analogues, and polyanionic compounds.[2−5] However, the mismatch of the thermodynamic stability between the anode and the electrolyte leads to an extremely unstable interphase whether on typical hard carbon (HC) anodes or Na metal anodes.

HC is considered to be the most promising anode material for SIBs due to its low operating voltage, high capacity, and low cost.[6] However, the long calendar life, rate capability, and initial Coulombic efficiency (ICE) are far from satisfactory. From the prospective of pursuing higher energy densities, the Na metal anode deserves to be refocused due to the high theoretical specific capacity (1166 mA h g^{-1}) and low redox potential (−2.714 V versus standard hydrogen electrode potential).[7] However, its reactivity is higher than that of hard carbon, which would aggravate the electrode−electrolyte interface and result in extremely low CEs in typical ester electrolytes. By building an anode-free battery, its energy density can be fully extracted to make it comparable to state-of-the-art LIBs. While harvesting ultrahigh energy density, it puts forward more stringent requirements for the stability of both cathode and anode interfaces. Obviously, the continued pursuit of high energy density comes with greater challenges. This Outlook comprehensively summarizes the basic scientific issues of anode electrodes from HCs to anode-free systems and generalizes and discusses the nanoconfining strategy in optimizing the desolvation process, as well as its impact on anode interphase stability (Figure 1).

2. HARD CARBON ANODES

Different from the stable interaction of Li^+ in graphite, the intercalation compounds formed by the intercalation of Na^+ are thermodynamically extremely unstable.[8] Therefore, the cheap graphite cannot be used as the anode for SIBs. However, HC is composed of randomly oriented and distorted graphene

Received: March 11, 2023
Published: May 15, 2023

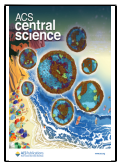

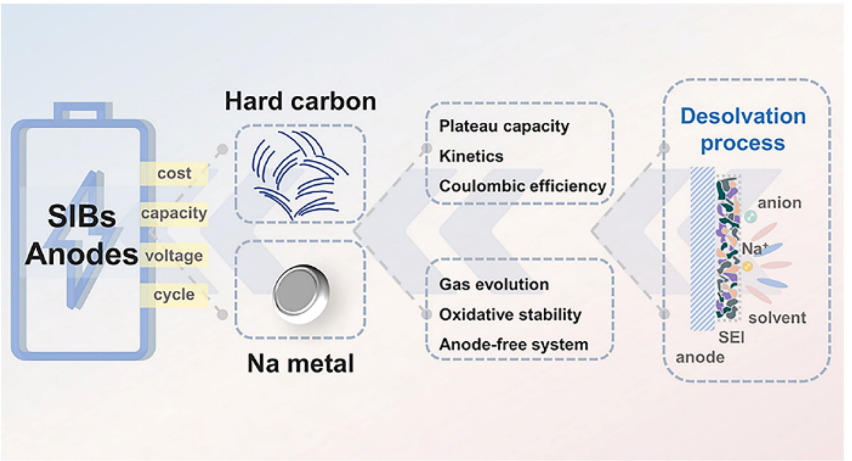

Figure 1. Schematic illustration of regulating the desolvation process to solve the problems of anode electrodes for SIBs.

nanosheets that generate randomly distributed graphitized microdomains pores or voids as active sites, which enables it to efficiently store sodium ion (Na^+).[9] Considering the narrow layer spacings of other carbon materials and the thermodynamic instability of products, which impeded Na storage, hard carbon materials have attracted general attention as anodes for sodium-ion batteries relying on the outstanding sodium storage performance, various raw materials, and low cost. In addition, owing to its unique advantages including low-cost, high abundance, high capacity, and low redox potential, hard carbon is regarded as the most ideal anode for SIBs.[10] The Na^+ storage mechanism in hard carbon is different from the Li^+ storage mechanism in graphite. Typical discharge curves of hard carbons exhibit distinct slope and plateau regions, which correspond to different Na^+ storage mechanisms. The slope region is generally attributed to the adsorption of Na^+ on the surface/defects or the insertion of Na^+ in few-layer graphene. The plateau region has been assigned to Na clustering in nanopores, which has a vital influence on the discharging capacity and average potential.[11−14] However, undesirable side reactions between HCs and electrolytes lead to the dissolution and reformation of the solid electrolyte interphase (SEI), resulting in increased impedance and decreased CE. Procedurally, the interfacial electric double layer (IEDL) formed by the adsorption of solvated Na^+ on negatively charged hard carbon plays a decisive role in interfacial electrochemistry.[15,16] Hence, the stability of the interface depends not only on the structural properties of hard carbon itself but also on the solvation configuration of the electrolyte.

The pore entrance size and pore body size of hard carbon have a crucial effect on the formation of Na clusters and the capacity of the low-potential plateau.

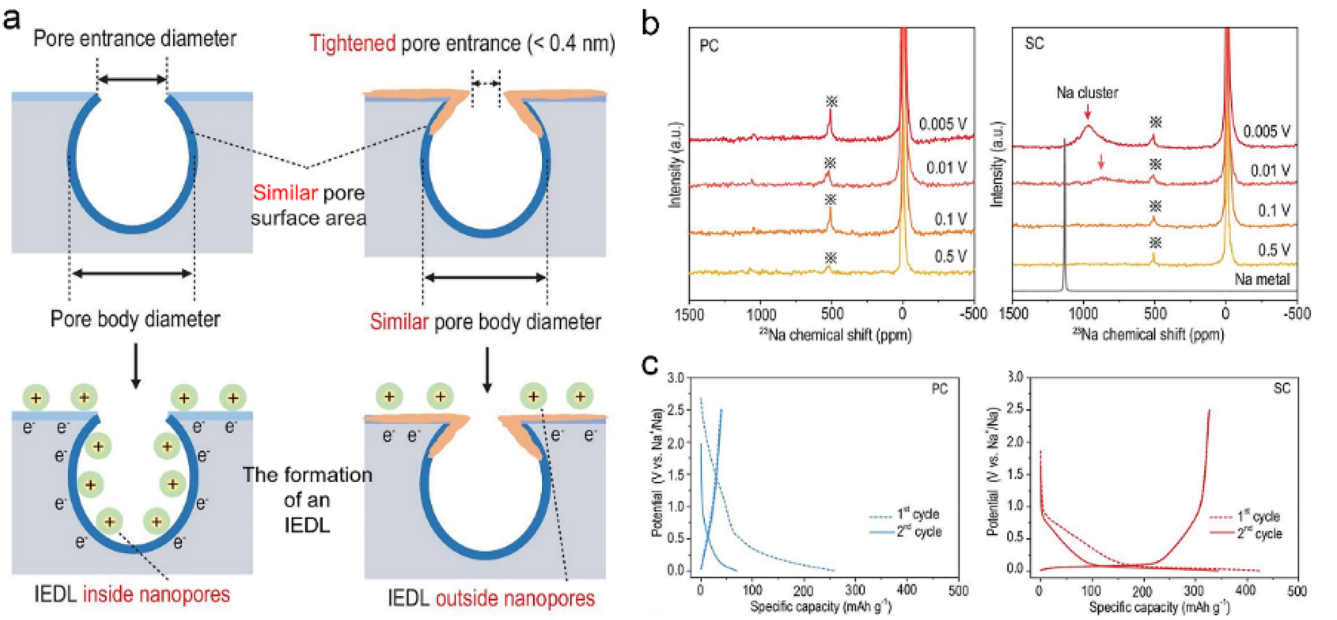

Figure 2. (a) Tightening the pore entrance and the comparison of IEDLs. (b) ^{23}Na MAS ssNMR spectra and (c) discharge/charge curves of porous carbon and sieving carbon. Reprinted from ref 16. Copyright 2022 The Authors. Published by Oxford University Press.

https://doi.org/10.1021/acscentsci.3c00301
ACS Cent. Sci. 2023, 9, 1076−1087

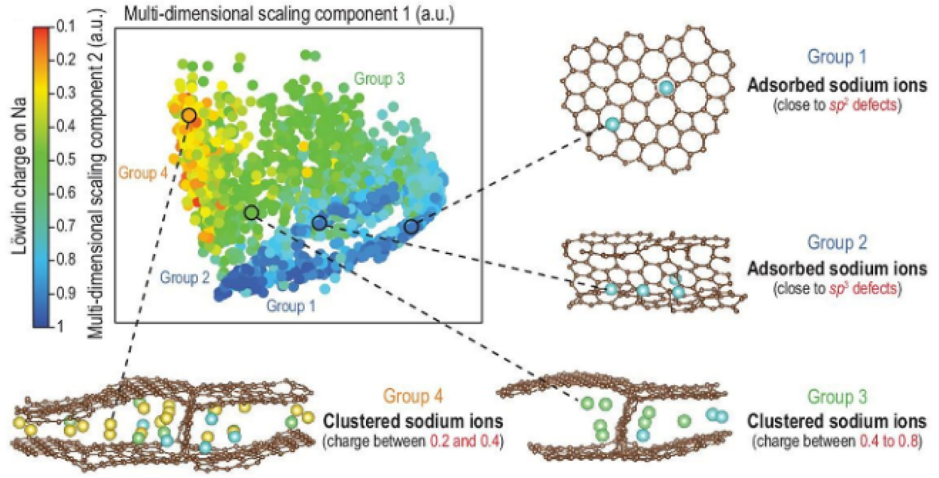

Figure 3. Analysis of the local environment of stored Na^+ in sieving carbons using a smooth overlap of atomic positions kernel as a structural similarity initially used for Gaussian approximation potential fitting. Reprinted from ref 16. Copyright 2022 The Authors. Published by Oxford University Press.

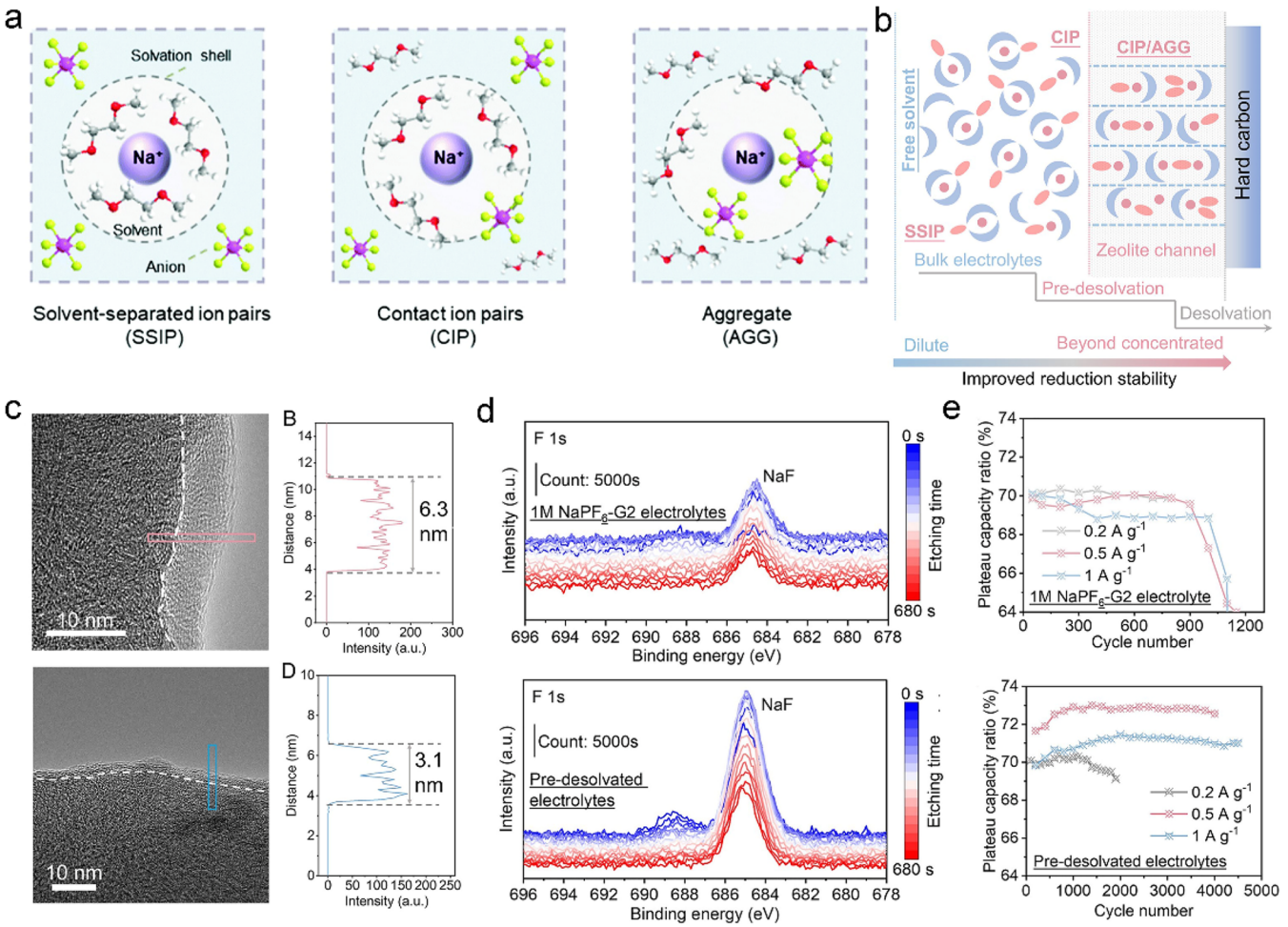

Figure 4. (a) Schematic diagram of the SSIP, CIP, and AGG.[61]. Reproduced with permission from ref 61. Copyright 2022 Royal Society of Chemistry. (b) Schematic diagram of the step-by-step desolvation process. Comparison of (c) the TEM image of hard carbon after 100 cycles, (d) Na fluoride (NaF) XPS signal changes, and (e) the variation of plateau capacity ratios of the pristine ether electrolytes and predesolvated electrolytes.[50] Reproduced from ref 50. Copyright 2022 The Authors. Published by PNAS.

2.1. Accurate Structural Design. In the past few decades, as a conventional strategy to enhance the performance, tuning the structure of HCs has attracted general attention. Precursor reagent screening,[17−20] optimizing synthesis conditions,[21−23] gradient design,[14,24,25] and heteroatom substitution[26−29] have been adopted to regulate specific characteristics including

https://doi.org/10.1021/acscentsci.3c00301
ACS Cent. Sci. 2023, 9, 1076−1087

defect concentration, specific surface area, and the degree of graphitization.[30,31] The pore and structural features of hard carbon itself are critical for electrolyte−electrode interface stability. Therefore, reconstructing the structural features of pores or voids is proposed as an effective strategy to construct a stable interphase and stabilize the hard carbon anode. The enhanced cycling stability and reaction kinetics of HCs have been achieved by precisely controlling the size of the nanopore. The feasibility of using commercial carbon molecular sieves with well-defined pore sizes as the anode materials of SIBs has been verified, providing a reversible capacity of ∼300 mA h g^{-1} at 100 mA g^{-1} and a high ICE of 73.2%.[32]

Subsequently, the pore entrance size of porous carbon was precisely tightened from micropores (>1 nm) to ultramicropores (0.3−0.5 nm) by Yang and co-workers.[16] Since the IEDL has a decisive influence on the interfacial electrochemistry and SEI formation, insulating solvent-associated molecules from entering nanopores is essential to promote the formation of a Na cluster in the plateau region (Figure 2a). Chemical vapor deposition (CVD) of methane is used to tighten the pore entrance diameter (PED, < 0.4 nm) and filter out the solvated Na^+ to shelter the Na clusters by accurate parameter control.[16] This precisely customized nanopore is accessible to the naked Na^+ so that the decomposition of electrolytes can be minimized and the interface stability is largely improved, which enables excellent rate and cycling performance as well as a high ICE (80.6%). In addition, the tightened pore entrance and selective body diameter induce suitable Na metallicity and prevent the side reactions between the electrolytes and Na clusters, which have been unraveled by in situ ^{23}Na magic-angle-spinning solid-state nuclear magnetic resonance (ssNMR) and operando Raman spectroscopy (Figure 2b). These carefully designed sieving carbons derived from porous carbon provide a plateau capacity over 400 mA h g^{-1} with attractive reversibility (Figure 2c).

In addition, machine learning provides insights into dynamic Na cluster formation and the prediction of Na^+ storage sites in sieving carbons (Figure 3). The simulations show that Na^+ aggregates and gradually evolves to quasi-metallic Na with increasing Na^+ insertion, which is very consistent with the results of ssNMR. This work highlights the effect of pore entrance size on Na cluster formation and plateau capacity. The related theoretical simulation, combined with experimental results, provides an invaluable reference for the materials design and mechanism analysis of HCs.

2.2. Electrolyte Manipulation. In addition to the intrinsic properties of hard carbons, the compatibility between the electrolyte and the derived SEI has been described as a critical factor that has a significant influence on the charge transfer kinetics.[33−36] This seriously jeopardizes battery performance, especially the rate capability. Many efforts have been made to address this issue, such as raw material screening,[37,38] heteroatom doping,[27,39] defect tuning,[40] and porous structure optimization.[12] Unfortunately, the majority of these works have obtained certain improvements at the expense of the low potential plateau (LPP) capacity decreasing. The amount of defects and specific surface areas are negatively correlated with the ICE but positively correlated with the reversible capacity.[41] The dilemma of the electrochemical capability enhancement of HCs has not been comprehensively resolved by material modification.

The theory of the solvation process can be summarized into three aspects, including the dissolution and solvation of Na^+, the migration of ionic groups, and the desolvation process.[42] Solvation structures usually include solvent-separated ion pairs (SSIPs), contact ion pairs (CIPs), and aggregates (AGGs) as solvates according to cation−anion interactions (Figure 4a). There are substantial efforts that have been made in solvation structure regulation to optimize the stability of the interphase.[43] For example, sodium difluoro(oxalate)borate (NaODFB) was synthesized and used in combination with dimethoxyethane (DME), which exhibits enhanced performance at high temperature by forming a special SEI component containing B−F and B−O inorganic groups.[44] Furthermore, the high-concentration electrolytes bring many benefits, such as anticorrosion perperties, cation transference, interfacial chemistries, and so on, relying on manufacturing solvation sheath structures.[45−47] Improved performance is also achieved by improving the SEI stability and uniformity using a weakly solvated electrolyte.[48,49] It is considered that the desolvation process presents a decisive effect on the Na^+ storage kinetics and the characteristics of SEIs.[50−53] In regard to the current status, more attention needs to be given to probe the rationale underneath the desolvation process.

Relying on the size effect and particular influence on the solvation structure, porous materials such as metal−organic frameworks (MOFs)[62] and zeolite molecular sieves (ZMS)[63,64] have been used to regulate the properties of electrolytes and exhibit unusual performances. Recently, a 3 Å ZMS film is introduced to transform the one-step desolvation process to the step-by-step desolvation process (Figure 4b).[50] Predesolvation by molecular sieves transforms SSIP-dominated solutions into highly aggregated electrolytes dominated by CIPs and AGGs. This extraordinary stepwise desolvation process adequately dispersed and reduced the high energy barriers of both the desolvation and the activation of Na^+ transport through the SEI. Additionally, a thin and inorganic-component-rich SEI was generated using the predesolvated electrolytes (Figure 4c). The high abundance of NaF in the SEI results in a very high modulus, which effectively guarantees the mechanical stability of the interphase (Figure 4d). Thereby, the life span and rate capability are dramatically improved, which is much better than using other strategies such as precursor reagent screening, optimization of synthesis conditions, gradient design, and heteroatom substitution (Table 1). What stands out is that the LPP capacity is well maintained with increased current densities, and a LPP capacity ratio of 73% can be maintained at a current density of 0.5 A g^{-1} (Figure 4e). It is worth noticing that this strategy shows excellent versatility, as the electrochemical performance of HC anodes was enhanced in both ester and ether electrolytes. It is generally believed that in ester electrolytes bare Na^+ is inserted into hard carbon after desolvation.[65,66] However, in ether electrolytes Na^+ and the solvated shell coinserted into hard carbons, which has faster reaction kinetics and a lower activation energy for desolvation.[54,61] This is an important reason why hard carbon anodes have better performance in ether electrolytes. The optimization of the desolvation process provides a novel perspective for facilitating the application of HC anodes.

3. NA METAL ANODES

3.1. Electrolyte Desolvation. *3.1.1. Ester-Based Electrolyte.* In response to the requirements of high energy density for the next generation of Na-based batteries, Na metal anodes hold great promise due to their high theoretical specific

https://doi.org/10.1021/acscentsci.3c00301
ACS Cent. Sci. 2023, 9, 1076−1087

Table 1. Comparison of the Stability and Cycle Number of Hard Carbon Anodes Using Different Strategies

electrolytes	current density (A/g)	cycle number	decay rate (%)	ref
Zeolite film modified	0.2	1900	0.0068	50
	0.5	4000	0.0015	
	1	4500	0.002	
HCM-1300-ZBE	2	3000	0.002	12
CMS	0.1	300	0.0372	17
CPs	0.5	500	0.02	18
BPC-11	2	3000	0.0133	19
S-HC-p	1	4000	0.005	29
HCNS	1	3000	0.0094	54
MV-HC	0.2	1100	0.015	40
HC-ether	1	2000	0.005	55
HCP	0.2	1000	0.007	56
HC-DME-0.5%VC	1	2000	0.0022	57
HC-0.5 M NaBPh4/ DME	1	1500	0.012	58
HC-Al2O3	1	2000	0.00655	59
HTCS-1000	1	1000	0.0197	60

The optimization of desolvation process has shown excellent versatility for enhancing the performance of hard carbon anodes.

capacity and low redox potential. The typical carbonate ester electrolytes generally have excellent antioxidative stability to match a high voltage cathode over 4.0 V. However, there is a strong chemical reactivity between Na metal and the ester electrolyte, leading to persistent parasitic reactions (Figure 5a).[67−70] When Na metal is in contact with the ester electrolyte, an obvious gas production reaction spontaneously occurs to release combustible gases (H_2 and alkanes, Figure 5b)[71,72] that would severely affect the stability of the Na metal anode, leading to extremely poor reversibility and a low CE. Unfavorable solid byproducts further facilitate the formation of fragile SEI and performance degradation.

Constructing protective layers on the surface of Na metal has been demonstrated to be effective.[73−80] For example, Yu and co-workers advocate that building a sodium bromide (NaBr) coating by the Wurtz reaction or the decomposition of a 1,2-dibromobenzene additive on the Na metal anode effectively reduces the interfacial ion-transport activation energy and restricts Na dendrite formation.[81] Besides, tuning the solvation structure via some additives, for example, 4-acetylpyridine, has been proposed as an effective strategy.[82] However, tailoring the desolvation process to stabilize the interface and suppress detrimental gas evolution has not been paid enough attention.

Generally, the solvent molecules show a reduced the lowest unoccupied molecular orbital (LUMO) after complexing with Na^+, which promotes the reductive decomposition of the electrolyte and leads to gas evolution and unfavorable SEIs.[71] Manipulating the solvent structure toward anion-mediated

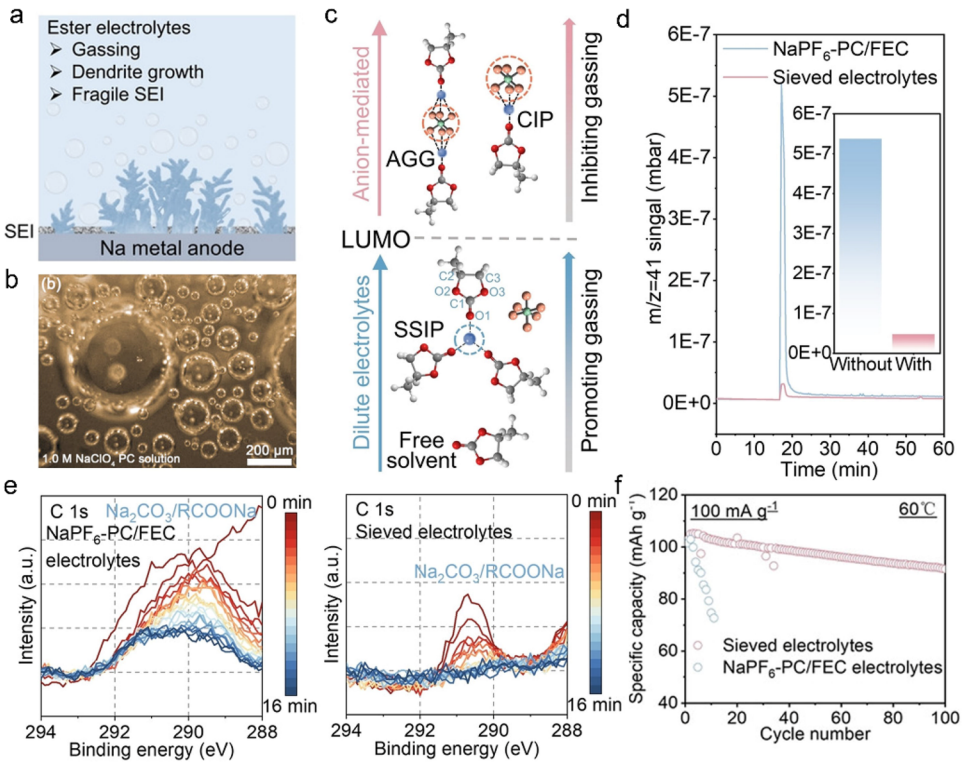

Figure 5. (a) Schematic showing of gassing-related byproducts[83]. Reproduced with permission from ref 83. Copyright 2022 Wiley-VCH. (b) In situ optical microscopic images of gas evolution of Na metal in PC-based electrolytes.[71] Reproduced with permission from ref 71. Copyright 2017 Wiley-VCH. (c) Relationship between solvation structures and gassing reactivity. (d) Mass signal of C_3H_6 (m/z = 41) after being immersed in Na. (e) Na_2CO_3 XPS signal depth profiles of the SEI formed. (f) Cycling stability of Na||NVPF cells at 60 °C in pristine 1 M sodium hexafluorophosphate ($NaPF_6$) in propylene carbonate (PC) as the solvent with 5% fluoroethylene carbonate (FEC) additive ($NaPF_6$−PC/FEC) electrolytes and sieved electrolytes.[83] Reproduced with permission from ref 83. Copyright 2022 Wiley-VCH.

https://doi.org/10.1021/acscentsci.3c00301
ACS Cent. Sci. 2023, 9, 1076−1087

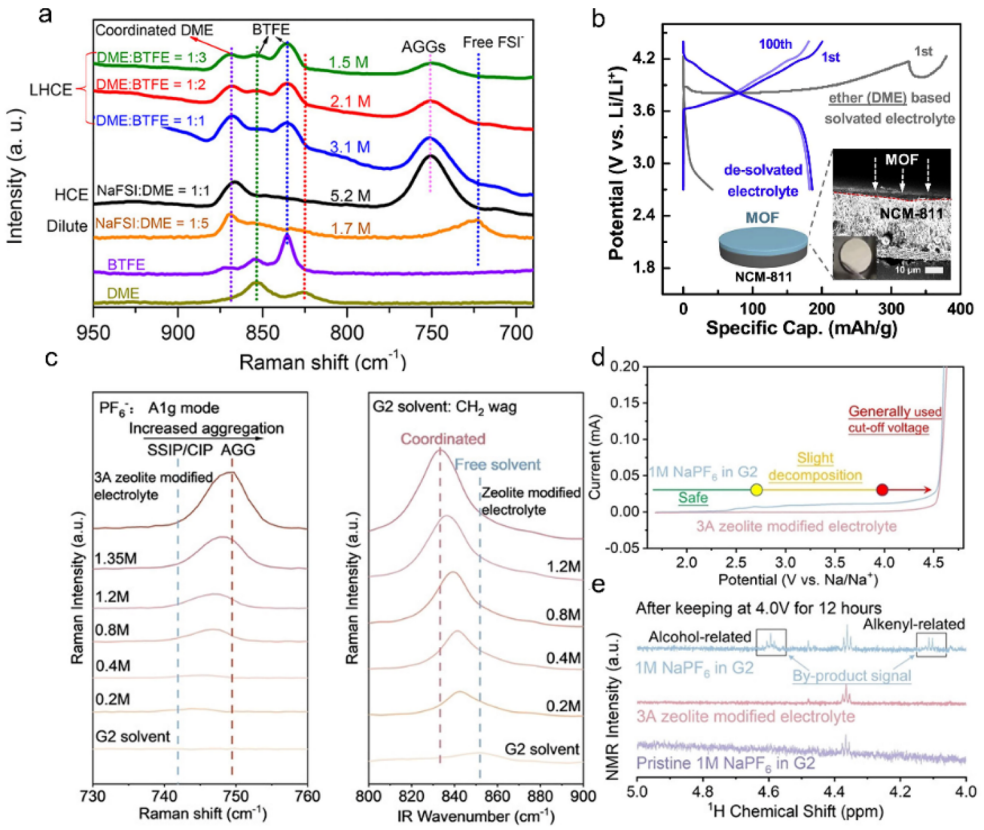

Figure 6. (a) Raman spectra of high-concentration electrolytes and localized high-concentration electrolytes with different sodium bis(fluorosulfonyl)imide (NaFSI) concentrations.[98] Reproduced with permission from ref 98. Copyright 2018 American Chemical Society. (b) Discharge/charge curves of the NCM-811//Li batteries using typical "Li^+ solvated ether-based electrolytes" (1 M lithium bis(trifluoromethanesulfonyl)imide (LiTFSI) in 1,3-dioxolane (DOL) and dimethoxyethane (DME), LiTFSI−DOL−DME) and the "Li^+ de-solvated electrolyte" (1 M Li^+ desolvated LiTFSI−DOL−DME).[94] Reproduced with permission from ref 94. Copyright 2020 Elsevier. (c) Raman and FT-IR spectra of various electrolytes. (d) Linear sweep cyclic voltammetry (LSV) tests and (e) ^{1}H NMR results of pristine 1 M $NaPF_6$−G2 electrolytes and 3A zeolite-modified electrolytes.[99] Reproduced with permission from ref 99. Copyright 2022 Wiley-VCH.

CIPs and AGGs can effectively increase the LUMO, thereby reducing side reactions and subsequent gassing (Figure 5c). This has been demonstrated as an effective strategy in high-concentrated electrolytes.[84−86] However, considering the cost of adding an additional dose of expensive sodium salt, it is of great significance to develop effective and economical methods to facilitate the regulation of the solvation structure. 3 Å ZMS film has been added into the assembly of Na metal batteries (SMBs) and placed between the Na metal and the separator manufacturing sieved electrolytes.[83] Relying on the size effect, the cation-dominated SSIP is blocked and CIP/AGG is successfully retained in the nanopore due to size effect, which is considered to be similar to superconcentrated electrolytes.[63,87] The significantly reduced electrolyte activity effectively suppresses the violent decomposition of metallic Na and the release of combustible gases (Figure 5d). In addition, a robust SEI with abundant NaF and Na_2O was identified, which has been shown to be beneficial for reversible Na plating and stripping. Carbonate-related byproducts are also efficiently suppressed, as demonstrated by X-ray photoelectron spectroscopy (XPS) (Figure 5e).[83] Finally, Na metal batteries with sieved electrolytes exhibited excellent electrochemical performance even under harsh conditions of high temperature (60 °C) (Figure 5f). This approach provides a new perspective for improving the performance of high-voltage Na metal batteries with ester-based electrolytes.

3.1.2. Ether-Based Electrolyte. Ether-based electrolytes have much better compatibility with Na metal anodes due to their excellent antireduction stability.[88] Nevertheless, the oxidation stability of ether-based electrolytes is far from satisfactory. Adjusting the solvation structure and composition of electrolytes by increasing the concentration has been shown to be effective to reduce the activity of the electrolyte and extend the operating voltage window.[86,89−91] A localized high-concentration electrolyte was constructed by Zhang et al. by introducing an inert diluent, which exhibited a high CE of 99% (Figure 6a). However, due to the low solubility of salts in ether solvents, it is crucial to explore additives, cosolvents, or other methods to tailor the solvation structure. Some cation additives have been explored and added to the electrolyte to modify the solvation structure and further enhance the electrolyte stability.[92,93] Recently, MOFs have been used to construct desolvated electrolytes for LIBs (Figure 6b), showing a promising effect in stabilizing a high-voltage cathode in ether electrolytes.[62,94−97] Therefore, adjusting the solvation structure via sieving effects holds great potential in enhancing the oxidative stability of ether-based electrolytes.

Applying the nanoconfining strategy, Lu et al. and co-workers achieved the regulation of the solvation structure by utilizing the molecular sieves with unique nanopore structures and showed dramatically improved oxidative stability.[99] Relying on the special size effect, highly aggregate solvation structures (CIP and AGG) are stored in the nanopore, which

https://doi.org/10.1021/acscentsci.3c00301
ACS Cent. Sci. 2023, 9, 1076−1087

The nanoconfining strategy in tuning the solvation structure and the desolvation process dramatically improved the performance of high-voltage Na metal batteries with ester-based electrolytes and the oxidation stability of ether-based electrolytes.

was verified by the comparison of the Raman and Fourier-transform infrared spectroscopy (FT-IR) signals of different concentrated and zeolite modified electrolytes (Figure 6c). The pristine 1 M $NaPF_6$−diglyme (G2) electrolytes undergo obvious decomposition, while the oxidation current of the modified electrolyte is negligible (Figure 6d). The oxidation byproducts such as alcohol-related and alkenyl-related species can be detected in 1 M $NaPF_6$−G2 electrolytes (Figure 6e). However, these signals are absent in zeolite-modified electrolytes. Thereby, the half cells of Na||$Na_3V_2(PO_4)_2F_3$ (NVPF) that used this modified electrolyte exhibited an impressive lifespan of more than 800 cycles with a broad voltage window up 2−4.25 V. This nanoconfining strategy by adjusting the solvation structure dramatically improves the oxidation stability ether-based electrolytes.

For all-solid-state electrolytes without applied organic electrolytes, it ensures high safety performance of the Na metal batteries. However, the space charge layer, the poor electrochemical/chemical interfacial stability, and the mechanical compatibility restrain the practical applications.[100,101] Furthermore, the generally used solid-state electrolytes such as sulfide-based[102,103] and polymer solid electrolytes[104] with high ion conductivity are unstable under high voltage. If these problems cannot be properly solved, it will be difficult to achieve the practical application of solid-state Na batteries.

3.2. Anode-Free Na Batteries. With the pursuit of ultimately improving mass and volume energy density, anode-

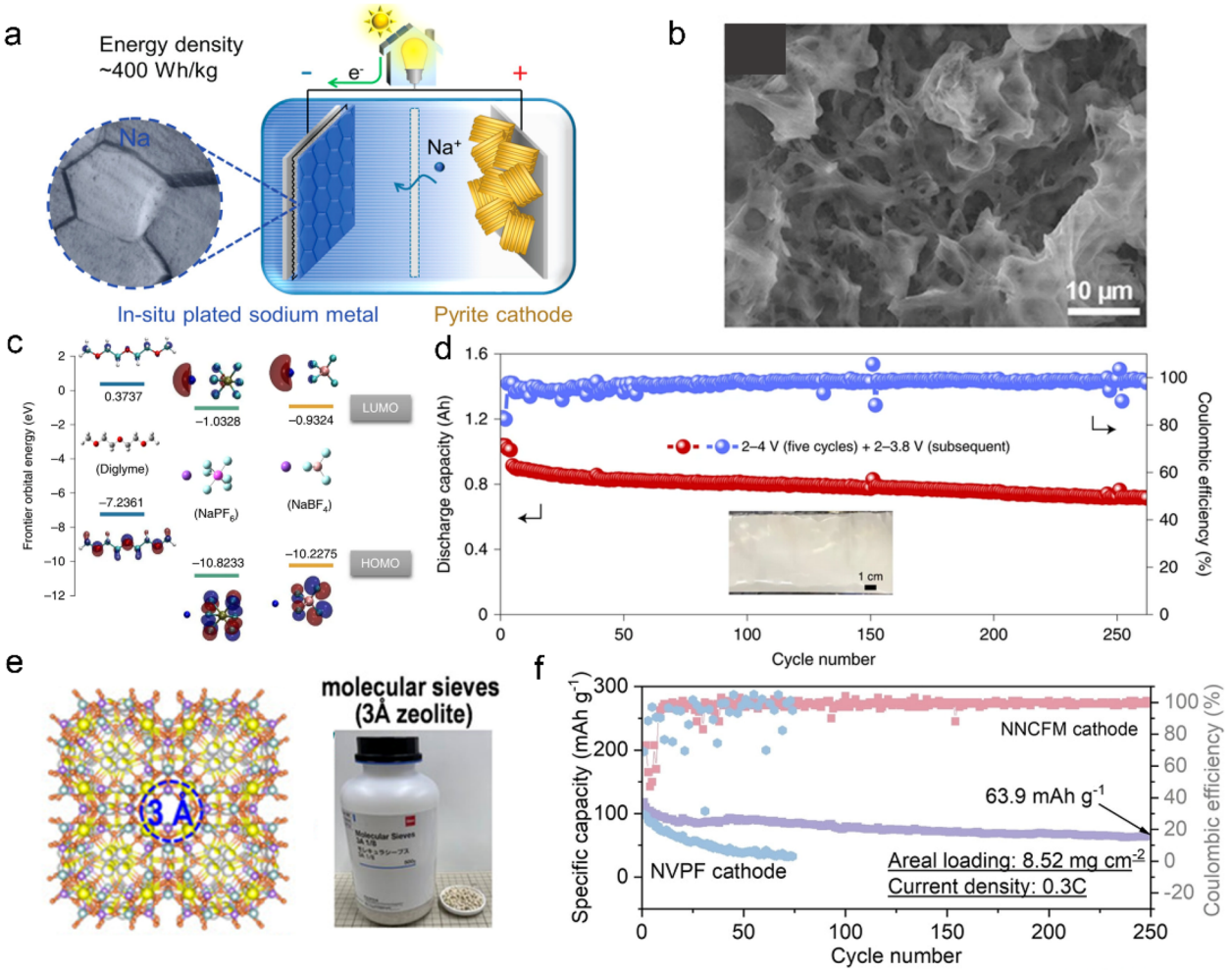

Figure 7. (a) Schematic illustration of an anode-free Na battery system.[112] Reproduced with permission from ref 112. Copyright 2017 American Chemical Society. (b) Top-view SEM images of the deposited Na on Cu foil using 1 M sodium perchlorate ($NaClO_4$) in ethylene carbonate (EC)/diethyl carbonate (DEC) + 5% FEC electrolytes.[113] Reproduced with permission from ref 113. Copyright 2022 Wiley-VCH. (c) LUMO and HOMO energies of $NaPF_6$, sodium tetrafluoroborate ($NaBF_4$), and diglyme. (d) Cyclic capability of the Ah-level cylindrical cell.[111] Reproduced with permission from ref 111. Copyright 2022 Nature Publishing Group. (e) Molecular sieve with 3 Å pore windows.[87] Reproduced with permission from ref 87. Copyright 2021 Wiley-VCH. (f) The cyclic stability of anode-free Al-$NaCu_{1/9}Ni_{2/9}Fe_{1/3}Mn_{1/3}O_2$ (NNCFM) full cells and Al−$Na_3V_2(PO_4)_2F_3$ (NVPF) full cells with 3A zeolite-modified electrolytes.[99] Reproduced with permission from ref 99. Copyright 2022 Wiley-VCH.

https://doi.org/10.1021/acscentsci.3c00301
ACS Cent. Sci. 2023, 9, 1076−1087

free Na batteries have attracted general attention due to their good economics and facile assembly procedure (Figure 7a). The generally used ester-based electrolytes shows outstanding oxidation stability to match a high-voltage cathode. However, the severe side reactions between Na metal and ester electrolytes and related gas evolution prevent the formation of a stable SEI, resulting in extremely low CE. Therefore, it is inapplicable in anode-free Na batteries (Figure 7b).[105−107] On the contrary, ether-based electrolytes have been reported to provide a high CE of over 99.9%.[88] The high reversibility of the Na metal anode in ether electrolytes can be attributed to two aspects. First, the ether electrolyte can generate a NaF- and Na_2O-dominated SEI, which effectively prevents the penetration of electrolyte and promotes the uniform Na metal deposition. Besides, the unique solvation structure for ether electrolytes enables a much lower activation energy for desolvation, which is favorable for the fast transport of Na^+ and guarantees the uniform deposition of Na metal.[35,108,109]

By using a 1 M $NaBF_4$−tetraglyme electrolyte, a reversible and smooth Na plating/stripping process is achieved, and the constructed $Na_2Fe_2(CN)_6$//Cu batteries show 76% capacity retention after 100 cycles.[110] Incorporating a graphitic carbon-coated current collector with a modified ether electrolyte (Figure 7c), Li et al. further increased the cycle life of the anode-free battery to 260 cycles at a charging cutoff voltage of 3.8 V (Figure 7d).[111] However, the cycling stability is severely compromised when the cutoff voltage is increase to 4.0 V. The current collector modification combined with the optimized electrolyte ensures the high reversibility of the Na anode. In this case, it is actually the high-voltage instability of the ether electrolyte that limits the lifespan.

Therefore, even using the-state-of -the-art ether electrolytes with an advanced current collector strategy such as the three-dimensional structural design of collectors[114−116] and the artificial sodiophilic layers,[117−122] the life span of an anode-free battery is generally limited within 100 cycles. Using highly concentrated electrolytes can improve the oxidation stability, and the CE will be greatly reduced at the same time.[94,123] In fact, as long as ether electrolytes are introduced, the oxidation stability would be an important factor limiting battery lifespan. Lu et al. significantly improved the antioxidation stability of the ether electrolyte by introducing a 3 Å ZMS (Figure 7e) film on the cathode, while the high CE of the Na anode was perfectly preserved. The Al−NVPF anode-free full cells operated stably at a cutoff voltage of 4.25 V. In addition, the Al|| $NaCu_{1/9}Ni_{2/9}Fe_{1/3}Mn_{1/3}O_2$ (Al−NNCFM) anode-free full cells delivered an immense energy density (2−4 V, 369 W h kg^{-1}) and a prolonged cycle life of 250 cycles (Figure 7f).[99] Tailoring the solvation structure of electrolytes by nanoconfining has shown its great potential for the development of anode-free Na batteries.

> Tailoring the electrolyte by nanoconfining strategy has shown great potential in the development of anode-free Na batteries.

As discussed above, there are two main factors affecting the life of an anode-free battery. First, the ultrahigh energy density relying on anode-free batteries needs the support of the high operating voltage. The high voltage stability of ether-based electrolytes may be enhanced by constructing dual or multisalt electrolytes or using fluorinated solvents, among others. Besides, even with a high CE of 99.9%, it preserves 36.8% of the pristine capacity after 1000 cycles, which is far from meeting the needs of practical applications. Using carbon materials or sodiophilic materials to promote the uniform nucleation and deposition of Na metal is promising to further increase the CE.

4. CONCLUSION AND OUTLOOK

SIBs are expected to play an important role in the development of distributed energy storage systems by virtue of their low cost and abundant raw materials. The stability of the anode−electrolyte interface has been a major stumbling block to the practicality of Na-based cells. We emphasize the size regulation of nanopores in hard carbon anodes and the role of nanoconfined electrolyte regulation in improving the interphase stability. Accurately tailoring the structure of hard carbons and tuning the desolvation process for porous materials are crucial in maintaining the LPP capacity. Furthermore, the nanoconfining strategy shows unexpected performance in inhibiting the gas evolution and oxidative decomposition. Although the nanoconfining strategy has achieved feasible effects, the fundamental mechanism and deeply comprehension have not been unraveled. Therefore, more attention should be paid to the following aspects.

4.1. Accurately Tailoring the Structure of HCs. Adjusting the desolvation process has shown tremendous potential in improving or maintaining the plateau capacity of HC anodes. It is crucial to establish the quantitative relation between the LPP capacity and the size of pores. The optimal sodiophilic pores or voids in HCs need to be explored to reach the limit of the LPP capacity. In addition, customizing electrolytes compatible with HCs is a feasible approach to address the stability of HC anodes.

4.2. Untangling the Mechanism of the Nanoconfining Strategy. The amelioration in inhibiting gassing and oxidative decomposition has been emphasized through the manipulation of the desolvation process by employing specific porous materials. The driving force for the solvated ions passing through the nonconducting films and related desolvation or predesolvation has not been identified. The interaction mechanism between nanoporous materials and solvated ions remains to be elucidated and verified. Besides, cracks of the film and gaps between particles are inevitable. In situ coating on the surface or cold rolling to fabricate the assisted films may be feasible methods.

4.3. Stepping Forward to Anode-Free Systems. The operating voltage of generally used cathodes such as layered oxides, Prussian blue analogues, and polyanion-type cathode are usually not lower than 4 V. Therefore, the focus of building an anode-free battery is the high voltage stability of the electrolyte. Under the premise of maintaining the high CE of the Na anode, the focus in designing a new type of electrolyte is to improve the high voltage stability. In addition, a CE of 99.9% is far from satisfactory for constructing stable anode-free cells. The integration of multiple strategies such as electrolyte optimization and current collector modification is an inevitable trend in the construction of practical anode-free batteries.

https://doi.org/10.1021/acscentsci.3c00301
ACS Cent. Sci. 2023, 9, 1076−1087

AUTHOR INFORMATION

Corresponding Authors

Ziyang Lu − *Graduate School of System and Information Engineering University of Tsukuba, Tsukuba, Ibaraki 305-8573, Japan; Energy Technology Research Institute, National Institute of Advanced Industrial Science and Technology (AIST), Tsukuba, Ibaraki 305-8568, Japan*; Email: Lu.ziyang@aist.go.jp

Haoshen Zhou − *College of Engineering and Applied Sciences, Jiangsu Key Laboratory of Artificial Functional Materials, National Laboratory of Solid State Microstructures, Collaborative Innovation Center of Advanced Microstructures, Nanjing University, Nanjing, Jiangsu 210093, China*; orcid.org/0000-0001-8112-3739; Email: hszhou@nju.edu.cn

Authors

Zhaoguo Liu − *College of Engineering and Applied Sciences, Jiangsu Key Laboratory of Artificial Functional Materials, National Laboratory of Solid State Microstructures, Collaborative Innovation Center of Advanced Microstructures, Nanjing University, Nanjing, Jiangsu 210093, China; Shenzhen Research Institute of Nanjing University, Shenzhen, Guangdong 518000, China*

Shaohua Guo − *College of Engineering and Applied Sciences, Jiangsu Key Laboratory of Artificial Functional Materials, National Laboratory of Solid State Microstructures, Collaborative Innovation Center of Advanced Microstructures, Nanjing University, Nanjing, Jiangsu 210093, China; Shenzhen Research Institute of Nanjing University, Shenzhen, Guangdong 518000, China*; orcid.org/0000-0003-0818-8354

Quan-Hong Yang − *Nanoyang Group, Tianjin Key Laboratory of Advanced Carbon and Electrochemical Energy Storage, and Collaborative Innovation Center of Chemical Science and Engineering (Tianjin), Tianjin University, Tianjin 300072, China*; orcid.org/0000-0003-2882-3968

Complete contact information is available at: https://pubs.acs.org/10.1021/acscentsci.3c00301

Notes

The authors declare no competing financial interest.

REFERENCES

(1) Yang, Z.; Zhang, J.; Kintner-Meyer, M. C.; Lu, X.; Choi, D.; Lemmon, J. P.; Liu, J. Electrochemical energy storage for green grid. *Chem. Rev.* **2011**, *111* (5), 3577−613.

(2) Jiang, K.; Xu, S.; Guo, S.; Zhang, X.; Zhang, X.; Qiao, Y.; Fang, T.; Wang, P.; He, P.; Zhou, H. A phase-transition-free cathode for sodium-ion batteries with ultralong cycle life. *Nano Energy* **2018**, *52*, 88−94.

(3) Jin, T.; Li, H.; Zhu, K.; Wang, P. F.; Liu, P.; Jiao, L. Polyanion-type cathode materials for sodium-ion batteries. *Chem. Soc. Rev.* **2020**, *49* (8), 2342−2377.

(4) Hirsh, H. S.; Li, Y.; Tan, D. H. S.; Zhang, M.; Zhao, E.; Meng, Y. S. Sodium-Ion Batteries Paving the Way for Grid Energy Storage. *Adv. Energy Mater.* **2020**, *10* (32), 2001274.

(5) Peng, J.; Zhang, W.; Liu, Q.; Wang, J.; Chou, S.; Liu, H.; Dou, S. Prussian Blue Analogues for Sodium-Ion Batteries: Past, Present, and Future. *Adv. Mater.* **2022**, *34* (15), 2108384.

(6) Chu, Y.; Zhang, J.; Zhang, Y.; Li, Q.; Jia, Y.; Dong, X.; Xiao, J.; Tao, Y.; Yang, Q. H. Reconfiguring Hard Carbons with Emerging Sodium-ion Batteries: a Perspective. *Adv. Mater.* **2023**, 2212186.

(7) Shi, P.; Zhang, S.; Lu, G.; Wang, L.; Jiang, Y.; Liu, F.; Yao, Y.; Yang, H.; Ma, M.; Ye, S.; Tao, X.; Feng, Y.; Wu, X.; Rui, X.; Yu, Y. Red Phosphorous-Derived Protective Layers with High Ionic Conductivity and Mechanical Strength on Dendrite-Free Sodium and Potassium Metal Anodes. *Adv. Energy Mater.* **2021**, *11* (5), 2003381.

(8) Xu, J.; Dou, Y.; Wei, Z.; Ma, J.; Deng, Y.; Li, Y.; Liu, H.; Dou, S. Recent Progress in Graphite Intercalation Compounds for Rechargeable Metal (Li, Na, K, Al)-Ion Batteries. *Adv. Sci. (Weinh)* **2017**, *4* (10), 1700146.

(9) Zhang, L.; Wang, W.; Lu, S.; Xiang, Y. Carbon Anode Materials: A Detailed Comparison between Na-ion and K-ion Batteries. *Adv. Energy Mater.* **2021**, *11* (11), 2003640.

(10) Yabuuchi, N.; Kubota, K.; Dahbi, M.; Komaba, S. Research development on sodium-ion batteries. *Chem. Rev.* **2014**, *114* (23), 11636−11682.

(11) Sun, N.; Qiu, J.; Xu, B. Understanding of Sodium Storage Mechanism in Hard Carbons: Ongoing Development under Debate. *Adv. Energy Mater.* **2022**, *12* (27), 2200715.

(12) Yin, X.; Lu, Z.; Wang, J.; Feng, X.; Roy, S.; Liu, X.; Yang, Y.; Zhao, Y.; Zhang, J. Enabling Fast Na^+ Transfer Kinetics in the Whole-Voltage-Region of Hard-Carbon Anodes for Ultrahigh-Rate Sodium Storage. *Adv. Mater.* **2022**, *34* (13), 2109282.

(13) Bin, D. S.; Xu, Y. S.; Guo, S. J.; Sun, Y. G.; Cao, A. M.; Wan, L. J. Manipulating Particle Chemistry for Hollow Carbon-based Nanospheres: Synthesis Strategies, Mechanistic Insights, and Electrochemical Applications. *Acc. Chem. Res.* **2021**, *54* (1), 221−231.

(14) Bin, D. S.; Li, Y.; Sun, Y. G.; Duan, S. Y.; Lu, Y.; Ma, J.; Cao, A.-M.; Hu, Y. S.; Wan, L.-J. Structural Engineering of Multishelled Hollow Carbon Nanostructures for High-Performance Na-Ion Battery Anode. *Adv. Energy Mater.* **2018**, *8* (26), 1800855.

(15) Zhou, Y.; Su, M.; Yu, X.; Zhang, Y.; Wang, J. G.; Ren, X.; Cao, R.; Xu, W.; Baer, D. R.; Du, Y.; Borodin, O.; Wang, Y.; Wang, X. L.; Xu, K.; Xu, Z.; Wang, C.; Zhu, Z. Real-time mass spectrometric characterization of the solid-electrolyte interphase of a lithium-ion battery. *Nat. Nanotechnol.* **2020**, *15* (3), 224−230.

(16) Li, Q.; Liu, X.; Tao, Y.; Huang, J.; Zhang, J.; Yang, C.; Zhang, Y.; Zhang, S.; Jia, Y.; Lin, Q.; Xiang, Y.; Cheng, J.; Lv, W.; Kang, F.; Yang, Y.; Yang, Q. H. Sieving carbons promise practical anodes with extensible low-potential plateaus for sodium batteries. *Natl. Sci. Rev.* **2022**, *9* (8), nwac084.

(17) Li, Y.; Hu, Y. S.; Qi, X.; Rong, X.; Li, H.; Huang, X.; Chen, L. Advanced sodium-ion batteries using superior low cost pyrolyzed anthracite anode: towards practical applications. *Energy Stor. Mater.* **2016**, *5*, 191−197.

(18) Zhu, Z.; Liang, F.; Zhou, Z.; Zeng, X.; Wang, D.; Dong, P.; Zhao, J.; Sun, S.; Zhang, Y.; Li, X. Expanded biomass-derived hard carbon with ultra-stable performance in sodium-ion batteries. *J. Mater. Chem. A* **2018**, *6* (4), 1513−1522.

(19) Chen, C.; Huang, Y.; Zhu, Y.; Zhang, Z.; Guang, Z.; Meng, Z.; Liu, P. Nonignorable Influence of Oxygen in Hard Carbon for Sodium Ion Storage. *ACS Sustainable Chem. Eng.* **2020**, *8* (3), 1497−1506.

(20) Chen, H.; Sun, N.; Zhu, Q.; Soomro, R. A.; Xu, B. Microcrystalline Hybridization Enhanced Coal-Based Carbon Anode for Advanced Sodium-Ion Batteries. *Adv. Sci.* **2022**, *9* (20), 2200023.

(21) Yang, L.; Hu, M.; Lv, Q.; Zhang, H.; Yang, W.; Lv, R. Salt and sugar derived high power carbon microspheres anode with excellent low-potential capacity. *Carbon* **2020**, *163*, 288−296.

(22) Zhen, Y.; Chen, Y.; Li, F.; Guo, Z.; Hong, Z.; Titirici, M. M. Ultrafast synthesis of hard carbon anodes for sodium-ion batteries. *Proc. Natl. Acad. Sci. U. S. A.* **2021**, *118* (42), e2111119118.

(23) Zhao, C.; Wang, Q.; Lu, Y.; Li, B.; Chen, L.; Hu, Y. S. High-temperature treatment induced carbon anode with ultrahigh Na storage capacity at low-voltage plateau. *Sci. Bull.* **2018**, *63* (17), 1125−1129.

(24) Hou, H.; Banks, C. E.; Jing, M.; Zhang, Y.; Ji, X. Carbon Quantum Dots and Their Derivative 3D Porous Carbon Frameworks

for Sodium-Ion Batteries with Ultralong Cycle Life. *Adv. Mater.* **2015**, *27* (47), 7861−7866.
(25) Xia, J. L.; Yan, D.; Guo, L. P.; Dong, X. L.; Li, W. C.; Lu, A. H. Hard Carbon Nanosheets with Uniform Ultra-micropores and Accessible Functional Groups Showing High Realistic Capacity and Superior Rate Performance for Sodium-Ion Storage. *Adv. Mater.* **2020**, *32* (21), 2000447.
(26) Kim, D.-Y.; Li, O. L.; Kang, J. Novel synthesis of highly phosphorus-doped carbon as an ultrahigh-rate anode for sodium ion batteries. *Carbon* **2020**, *168*, 448−457.
(27) Huang, H.; Xu, R.; Feng, Y.; Zeng, S.; Jiang, Y.; Wang, H.; Luo, W.; Yu, Y. Sodium/Potassium-Ion Batteries: Boosting the Rate Capability and Cycle Life by Combining Morphology, Defect and Structure Engineering. *Adv. Mater.* **2020**, *32* (8), 1904320.
(28) Li, Z.; Bommier, C.; Chong, Z. S.; Jian, Z.; Surta, T. W.; Wang, X.; Xing, Z.; Neuefeind, J. C.; Stickle, W. F.; Dolgos, M.; Greaney, P. A.; Ji, X. Mechanism of Na-Ion Storage in Hard Carbon Anodes Revealed by Heteroatom Doping. *Adv. Energy Mater.* **2017**, *7* (18), 1602894.
(29) Hong, Z.; Zhen, Y.; Ruan, Y.; Kang, M.; Zhou, K.; Zhang, J. M.; Huang, Z.; Wei, M. Rational Design and General Synthesis of S-Doped Hard Carbon with Tunable Doping Sites toward Excellent Na-Ion Storage Performance. *Adv. Mater.* **2018**, *30*, 1802035.
(30) Winter, M.; Barnett, B.; Xu, K. Before Li Ion Batteries. *Chem. Rev.* **2018**, *118* (23), 11433−11456.
(31) Zhang, J.; Li, Q.; Tao, Y.; Yang, Q. Sieving carbons for sodium-ion batteries: Origin and progress. *Energy Storage Sci. Technol.* **2022**, *11* (9), 2825−2833.
(32) Zhang, S.-W.; Lv, W.; Luo, C.; You, C.-H.; Zhang, J.; Pan, Z.-Z.; Kang, F.-Y.; Yang, Q.-H. Commercial carbon molecular sieves as a high-performance anode for sodium-ion batteries. *Energy Stor. Mater.* **2016**, *3*, 18−23.
(33) Yang, J.; Wang, X.; Dai, W.; Lian, X.; Cui, X.; Zhang, W.; Zhang, K.; Lin, M.; Zou, R.; Loh, K. P.; Yang, Q. H.; Chen, W. From Micropores to Ultra-micropores inside Hard Carbon: Toward Enhanced Capacity in Room-/Low-Temperature Sodium-Ion Storage. *Nano-Micro Lett.* **2021**, *13*, 98.
(34) Zhang, M.; Li, Y.; Wu, F.; Bai, Y.; Wu, C. Boost sodium-ion batteries to commercialization: Strategies to enhance initial Coulombic efficiency of hard carbon anode. *Nano Energy* **2021**, *82*, 105738.
(35) Lv, Z.; Li, T.; Hou, X.; Wang, C.; Zhang, H.; Yan, J.; Zheng, Q.; Li, X. Solvation structure and solid electrolyte interface engineering for excellent Na+ storage performances of hard carbon with the ether-based electrolytes. *Chem. Eng. J.* **2022**, *430*, 133143.
(36) Meng, Y. S.; Srinivasan, V.; Xu, K. Designing better electrolytes. *Science* **2022**, *378* (6624), eabq3750.
(37) Yu, K.; Wang, X.; Yang, H.; Bai, Y.; Wu, C. Insight to defects regulation on sugarcane waste-derived hard carbon anode for sodium-ion batteries. *J. Energy Chem.* **2021**, *55*, 499−508.
(38) Li, Y.; Lu, Y.; Meng, Q.; Jensen, A. C. S.; Zhang, Q.; Zhang, Q.; Tong, Y.; Qi, Y.; Gu, L.; Titirici, M. M.; Hu, Y. S. Regulating Pore Structure of Hierarchical Porous Waste Cork-Derived Hard Carbon Anode for Enhanced Na Storage Performance. *Adv. Energy Mater.* **2019**, *9* (48), 1902852.
(39) Xie, F.; Niu, Y.; Zhang, Q.; Guo, Z.; Hu, Z.; Zhou, Q.; Xu, Z.; Li, Y.; Yan, R.; Lu, Y.; Titirici, M. M.; Hu, Y. S. Screening Heteroatom Configurations for Reversible Sloping Capacity Promises High-Power Na-Ion Batteries. *Angew. Chem., Int. Ed.* **2022**, *61* (11), e202116394.
(40) Li, Z.; Chen, Y.; Jian, Z.; Jiang, H.; Razink, J. J.; Stickle, W. F.; Neuefeind, J. C.; Ji, X. Defective Hard Carbon Anode for Na-Ion Batteries. *Chem. Mater.* **2018**, *30* (14), 4536−4542.
(41) Liu, M.; Wang, Y.; Wu, F.; Bai, Y.; Li, Y.; Gong, Y.; Feng, X.; Li, Y.; Wang, X.; Wu, C. Advances in Carbon Materials for Sodium and Potassium Storage. *Adv. Funct. Mater.* **2022**, *32* (31), 2203117.
(42) Tian, Z.; Zou, Y.; Liu, G.; Wang, Y.; Yin, J.; Ming, J.; Alshareef, H. N. Electrolyte Solvation Structure Design for Sodium Ion Batteries. *Adv. Sci.* **2022**, *9* (22), 2201207.
(43) Fondard, J.; Irisarri, E.; Courrèges, C.; Palacin, M. R.; Ponrouch, A.; Dedryvère, R. SEI Composition on Hard Carbon in Na-Ion Batteries After Long Cycling: Influence of Salts (NaPF6, NaTFSI) and Additives (FEC, DMCF). *J. Electrochem. Soc.* **2020**, *167* (7), No. 070526.
(44) Zhao, D.; Lu, H.; Li, S.; Wang, P.; Fan, X. Boosting the cycling stability of hard carbon with NaODFB-based electrolyte at high temperature. *Mater. Today Chem.* **2022**, *24*, 100866.
(45) Wang, J.; Yamada, Y.; Sodeyama, K.; Watanabe, E.; Takada, K.; Tateyama, Y.; Yamada, A. Fire-extinguishing organic electrolytes for safe batteries. *Nat. Energy* **2018**, *3* (1), 22−29.
(46) Takada, K.; Yamada, Y.; Watanabe, E.; Wang, J.; Sodeyama, K.; Tateyama, Y.; Hirata, K.; Kawase, T.; Yamada, A. Unusual Passivation Ability of Superconcentrated Electrolytes toward Hard Carbon Negative Electrodes in Sodium-Ion Batteries. *ACS Appl. Mater. Interfaces* **2017**, *9* (39), 33802−33809.
(47) Yamada, Y.; Wang, J.; Ko, S.; Watanabe, E.; Yamada, A. Advances and issues in developing salt-concentrated battery electrolytes. *Nat. Energy* **2019**, *4* (4), 269−280.
(48) Tang, Z.; Wang, H.; Wu, P. F.; Zhou, S. Y.; Huang, Y. C.; Zhang, R.; Sun, D.; Tang, Y. G.; Wang, H. Y. Electrode-Electrolyte Interfacial Chemistry Modulation for Ultra-High Rate Sodium-Ion Batteries. *Angew. Chem., Int. Ed.* **2022**, *61* (18), e202200475.
(49) Jin, Y.; Le, P. M. L.; Gao, P.; Xu, Y.; Xiao, B.; Engelhard, M. H.; Cao, X.; Vo, T. D.; Hu, J.; Zhong, L.; Matthews, B. E.; Yi, R.; Wang, C.; Li, X.; Liu, J.; Zhang, J.-G. Low-solvation electrolytes for high-voltage sodium-ion batteries. *Nat. Energy* **2022**, *7* (8), 718−725.
(50) Lu, Z.; Geng, C.; Yang, H.; He, P.; Wu, S.; Yang, Q. H.; Zhou, H. Step-by-step desolvation enables high-rate and ultra-stable sodium storage in hard carbon anodes. *Proc. Natl. Acad. Sci. U.S.A.* **2022**, *119* (40), e2210203119.
(51) Yi, X.; Li, X.; Zhong, J.; Wang, S.; Wang, Z.; Guo, H.; Wang, J.; Yan, G. Unraveling the Mechanism of Different Kinetics Performance between Ether and Carbonate Ester Electrolytes in Hard Carbon Electrode. *Adv. Funct. Mater.* **2022**, *32* (48), 2209523.
(52) Deng, L.; Goh, K.; Yu, F. D.; Xia, Y.; Jiang, Y. S.; Ke, W.; Han, Y.; Que, L. F.; Zhou, J.; Wang, Z. B. Self-optimizing weak solvation effects achieving faster low-temperature charge transfer kinetics for high-voltage Na3V2(PO4)2F3 cathode. *Energy Stor. Mater.* **2022**, *44*, 82−92.
(53) Zhang, J.; Wang, D. W.; Lv, W.; Zhang, S.; Liang, Q.; Zheng, D.; Kang, F.; Yang, Q. H. Achieving superb sodium storage performance on carbon anodes through an ether-derived solid electrolyte interphase. *Energy Environ. Sci.* **2017**, *10* (1), 370−376.
(54) Dong, R.; Zheng, L.; Bai, Y.; Ni, Q.; Li, Y.; Wu, F.; Ren, H.; Wu, C. Elucidating the Mechanism of Fast Na Storage Kinetics in Ether Electrolytes for Hard Carbon Anodes. *Adv. Mater.* **2021**, *33* (36), 2008810.
(55) He, Y.; Bai, P.; Gao, S.; Xu, Y. Marriage of an Ether-Based Electrolyte with Hard Carbon Anodes Creates Superior Sodium-Ion Batteries with High Mass Loading. *ACS Appl. Mater. Interfaces* **2018**, *10* (48), 41380−41388.
(56) Hou, B. H.; Wang, Y. Y.; Ning, Q. L.; Li, W. H.; Xi, X. T.; Yang, X.; Liang, H. J.; Feng, X.; Wu, X. L. Self-Supporting, Flexible, Additive-Free, and Scalable Hard Carbon Paper Self-Interwoven by 1D Microbelts: Superb Room/Low-Temperature Sodium Storage and Working Mechanism. *Adv. Mater.* **2019**, *31* (40), 1903125.
(57) Bai, P.; Han, X.; He, Y.; Xiong, P.; Zhao, Y.; Sun, J.; Xu, Y. Solid electrolyte interphase manipulation towards highly stable hard carbon anodes for sodium ion batteries. *Energy Stor. Mater.* **2020**, *25*, 324−333.
(58) Morikawa, Y.; Yamada, Y.; Doi, K.; Nishimura, S.i.; Yamada, A. Reversible and High-rate Hard Carbon Negative Electrodes in a Fluorine-free Sodium-salt Electrolyte. *Electrochemistry* **2020**, *88* (3), 151−156.
(59) Yu, C.; Li, Y.; Ren, H.; Qian, J.; Wang, S.; Feng, X.; Liu, M.; Bai, Y.; Wu, C. Engineering homo-type heterojunctions in hard carbon to induce stable solid electrolyte interfaces for sodium-ion batteries. *Carbon Energy* **2023**, *5* (1), e220.

https://doi.org/10.1021/acscentsci.3c00301
ACS Cent. Sci. 2023, 9, 1076−1087

(60) Zhong, W.; Cheng, D.; Zhang, M.; Zuo, H.; Miao, L.; Li, Z.; Qiu, G.; Cheng, A.; Zhang, H. Boosting ultrafast and durable sodium storage of hard carbon electrode with graphite nanoribbons. *Carbon* **2022**, *198*, 278−288.
(61) Li, Y.; Wu, F.; Li, Y.; Liu, M.; Feng, X.; Bai, Y.; Wu, C. Ether-based electrolytes for sodium ion batteries. *Chem. Soc. Rev.* **2022**, *51* (11), 4484−4536.
(62) Chang, Z.; Qiao, Y.; Yang, H.; Deng, H.; Zhu, X.; He, P.; Zhou, H. Beyond the concentrated electrolyte: further depleting solvent molecules within a Li+ solvation sheath to stabilize high-energy-density lithium metal batteries. *Energy Environ. Sci.* **2020**, *13* (11), 4122−4131.
(63) Li, Z.; Zhou, S.; Wu, X.; Zhang, B.; Yu, X.; Pei, F.; Liao, H. G.; Qiao, Y.; Zhou, H.; Sun, S. G. Restraining Shuttle Effect in Rechargeable Batteries by Multifunctional Zeolite Coated Separator. *Adv. Funct. Mater.* **2023**, *33* (8), 2211774.
(64) Yang, H.; Qiao, Y.; Chang, Z.; Deng, H.; Zhu, X.; Zhu, R.; Xiong, Z.; He, P.; Zhou, H. Reducing Water Activity by Zeolite Molecular Sieve Membrane for Long-Life Rechargeable Zinc Battery. *Adv. Mater.* **2021**, *33* (38), 2102415.
(65) Liu, Q.; Xu, R.; Mu, D.; Tan, G.; Gao, H.; Li, N.; Chen, R.; Wu, F. Progress in electrolyte and interface of hard carbon and graphite anode for sodium-ion battery. *Carbon Energy* **2022**, *4* (3), 458−479.
(66) Bommier, C.; Surta, T. W.; Dolgos, M.; Ji, X. New Mechanistic Insights on Na-Ion Storage in Nongraphitizable Carbon. *Nano Lett.* **2015**, *15* (9), 5888−5892.
(67) Sun, B.; Xiong, P.; Maitra, U.; Langsdorf, D.; Yan, K.; Wang, C.; Janek, J.; Schroder, D.; Wang, G. Design Strategies to Enable the Efficient Use of Sodium Metal Anodes in High-Energy Batteries. *Adv. Mater.* **2020**, *32* (18), 1903891.
(68) Zheng, X.; Bommier, C.; Luo, W.; Jiang, L.; Hao, Y.; Huang, Y. Sodium metal anodes for room-temperature sodium-ion batteries: Applications, challenges and solutions. *Energy Stor. Mater.* **2019**, *16*, 6−23.
(69) Lee, B.; Paek, E.; Mitlin, D.; Lee, S. W. Sodium Metal Anodes: Emerging Solutions to Dendrite Growth. *Chem. Rev.* **2019**, *119* (8), 5416−5460.
(70) Zhao, C.; Lu, Y.; Yue, J.; Pan, D.; Qi, Y.; Hu, Y.-S.; Chen, L. Advanced Na metal anodes. *J. Energy Chem.* **2018**, *27* (6), 1584−1596.
(71) Chen, X.; Shen, X.; Li, B.; Peng, H. J.; Cheng, X. B.; Li, B. Q.; Zhang, X. Q.; Huang, J. Q.; Zhang, Q. Ion-Solvent Complexes Promote Gas Evolution from Electrolytes on a Sodium Metal Anode. *Angew. Chem., Int. Ed. Engl.* **2018**, *57* (3), 734−737.
(72) Zhang, L.; Tsolakidou, C.; Mariyappan, S.; Tarascon, J.-M.; Trabesinger, S. Unraveling gas evolution in sodium batteries by online electrochemical mass spectrometry. *Energy Stor. Mater.* **2021**, *42*, 12−21.
(73) Rodriguez, R.; Loeffler, K. E.; Nathan, S. S.; Sheavly, J. K.; Dolocan, A.; Heller, A.; Mullins, C. B. In Situ Optical Imaging of Sodium Electrodeposition: Effects of Fluoroethylene Carbonate. *ACS Energy Lett.* **2017**, *2* (9), 2051−2057.
(74) Liu, X.; Zheng, X.; Dai, Y.; Wu, W.; Huang, Y.; Fu, H.; Huang, Y.; Luo, W. Fluoride-Rich Solid-Electrolyte-Interface Enabling Stable Sodium Metal Batteries in High-Safe Electrolytes. *Adv. Funct. Mater.* **2021**, *31* (30), 2103522.
(75) Lee, Y.; Lee, J.; Lee, J.; Kim, K.; Cha, A.; Kang, S.; Wi, T.; Kang, S. J.; Lee, H. W.; Choi, N. S. Fluoroethylene Carbonate-Based Electrolyte with 1 M Sodium Bis(fluorosulfonyl)imide Enables High-Performance Sodium Metal Electrodes. *ACS Appl. Mater. Interfaces* **2018**, *10* (17), 15270−15280.
(76) Liu, Y.; Jiang, R.; Xiang, H.; Huang, Z.; Yu, Y. 3-Trimethylsilyl-2-oxazolidinone, as a multifunctional additive to stabilize FEC-containing electrolyte for sodium metal batteries. *Electrochim. Acta* **2022**, *425*, 140746.
(77) Lu, Y.; Zhang, Q.; Han, M.; Chen, J. Stable Na plating/stripping electrochemistry realized by a 3D Cu current collector with thin nanowires. *Chem. Commun. (Cambridge, U. K.)* **2017**, *53* (96), 12910−12913.
(78) Wang, S.; Cai, W.; Sun, Z.; Huang, F.; Jie, Y.; Liu, Y.; Chen, Y.; Peng, B.; Cao, R.; Zhang, G.; Jiao, S. Stable cycling of Na metal anodes in a carbonate electrolyte. *Chem. Commun. (Cambridge, U. K.)* **2019**, *55* (95), 14375−14378.
(79) Luo, W.; Lin, C. F.; Zhao, O.; Noked, M.; Zhang, Y.; Rubloff, G. W.; Hu, L. Ultrathin Surface Coating Enables the Stable Sodium Metal Anode. *Adv. Energy Mater.* **2017**, *7* (2), 1601526.
(80) Zhao, Y.; Goncharova, L. V.; Zhang, Q.; Kaghazchi, P.; Sun, Q.; Lushington, A.; Wang, B.; Li, R.; Sun, X. Inorganic-Organic Coating via Molecular Layer Deposition Enables Long Life Sodium Metal Anode. *Nano Lett.* **2017**, *17* (9), 5653−5659.
(81) Wang, L.; Ren, N.; Yao, Y.; Yang, H.; Jiang, W.; He, Z.; Jiang, Y.; Jiao, S.; Song, L.; Wu, X.; Wu, Z. S.; Yu, Y. Designing Solid Electrolyte Interfaces towards Homogeneous Na Deposition: Theoretical Guidelines for Electrolyte Additives and Superior High-Rate Cycling Stability. *Angew. Chem., Int. Ed. Engl.* **2023**, *62* (6), e202214372.
(82) Wang, H.; Zhu, C.; Liu, J.; Qi, S.; Wu, M.; Huang, J.; Wu, D.; Ma, J. Formation of NaF-Rich Solid Electrolyte Interphase on Na Anode through Additive-Induced Anion-Enriched Structure of Na+ Solvation. *Angew. Chem., Int. Ed.* **2022**, *61* (38), e202208506.
(83) Lu, Z.; Yang, H.; Guo, Y.; He, P.; Wu, S.; Yang, Q. H.; Zhou, H. Electrolyte Sieving Chemistry in Suppressing Gas Evolution of Sodium-Metal Batteries. *Angew. Chem., Int. Ed.* **2022**, *61* (30), e202206340.
(84) Lee, J.; Lee, Y.; Lee, J.; Lee, S. M.; Choi, J. H.; Kim, H.; Kwon, M. S.; Kang, K.; Lee, K. T.; Choi, N. S. Ultraconcentrated Sodium Bis(fluorosulfonyl)imide-Based Electrolytes for High-Performance Sodium Metal Batteries. *ACS Appl. Mater. Interfaces* **2017**, *9* (4), 3723−3732.
(85) Seo, D. M.; Borodin, O.; Balogh, D.; O'Connell, M.; Ly, Q.; Han, S.-D.; Passerini, S.; Henderson, W. A. Electrolyte Solvation and Ionic Association III. Acetonitrile-Lithium Salt Mixtures−Transport Properties. *J. Electrochem. Soc.* **2013**, *160* (8), A1061−A1070.
(86) Yamada, Y.; Furukawa, K.; Sodeyama, K.; Kikuchi, K.; Yaegashi, M.; Tateyama, Y.; Yamada, A. Unusual stability of acetonitrile-based superconcentrated electrolytes for fast-charging lithium-ion batteries. *J. Am. Chem. Soc.* **2014**, *136* (13), 5039−5046.
(87) Chang, Z.; Qiao, Y.; Yang, H.; Cao, X.; Zhu, X.; He, P.; Zhou, H. Sustainable Lithium-Metal Battery Achieved by a Safe Electrolyte Based on Recyclable and Low-Cost Molecular Sieve. *Angew. Chem., Int. Ed. Engl.* **2021**, *60* (28), 15572−15581.
(88) Seh, Z. W.; Sun, J.; Sun, Y.; Cui, Y. A Highly Reversible Room-Temperature Sodium Metal Anode. *ACS Cent. Sci.* **2015**, *1* (8), 449−455.
(89) Chen, S.; Zheng, J.; Mei, D.; Han, K. S.; Engelhard, M. H.; Zhao, W.; Xu, W.; Liu, J.; Zhang, J. G. High-Voltage Lithium-Metal Batteries Enabled by Localized High-Concentration Electrolytes. *Adv. Mater.* **2018**, *30* (21), 1706102.
(90) Suo, L.; Borodin, O.; Gao, T.; Olguin, M.; Ho, J.; Fan, X.; Luo, C.; Wang, C.; Xu, K. "Water-in-salt" electrolyte enables high-voltage aqueous lithium-ion chemistries. *Science* **2015**, *350* (6263), 938−943.
(91) He, J.; Bhargav, A.; Shin, W.; Manthiram, A. Stable Dendrite-Free Sodium-Sulfur Batteries Enabled by a Localized High-Concentration Electrolyte. *J. Am. Chem. Soc.* **2021**, *143* (48), 20241−20248.
(92) Chen, X.; Shen, X.; Hou, T. Z.; Zhang, R.; Peng, H. J.; Zhang, Q. Ion-Solvent Chemistry-Inspired Cation-Additive Strategy to Stabilize Electrolytes for Sodium-Metal Batteries. *Chem.* **2020**, *6* (9), 2242−2256.
(93) Li, H.; Murayama, M.; Ichitsubo, T. Dendrite-free alkali metal electrodeposition from contact-ion-pair state induced by mixing alkaline earth cation. *Cell Rep. Phys. Sci.* **2022**, *3* (6), 100907.
(94) Chang, Z.; Qiao, Y.; Deng, H.; Yang, H.; He, P.; Zhou, H. A Liquid Electrolyte with De-Solvated Lithium Ions for Lithium-Metal Battery. *Joule* **2020**, *4* (8), 1776−1789.
(95) Bhide, A.; Hofmann, J.; Dürr, A. K.; Janek, J.; Adelhelm, P. Electrochemical stability of non-aqueous electrolytes for sodium-ion

https://doi.org/10.1021/acscentsci.3c00301
ACS Cent. Sci. 2023, 9, 1076−1087

batteries and their compatibility with Na0.7CoO2. *Phys. Chem. Chem. Phys.* **2014**, *16* (5), 1987−1998.
(96) Morales, D.; Ruther, R. E.; Nanda, J.; Greenbaum, S. Ion transport and association study of glyme-based electrolytes with lithium and sodium salts. *Electrochim. Acta* **2019**, *304*, 239−245.
(97) Chang, Z.; Yang, H.; Qiao, Y.; Zhu, X.; He, P.; Zhou, H. Tailoring the Solvation Sheath of Cations by Constructing Electrode Front-Faces for Rechargeable Batteries. *Adv. Mater.* **2022**, *34* (34), 2201339.
(98) Zheng, J.; Chen, S.; Zhao, W.; Song, J.; Engelhard, M. H.; Zhang, J.-G. Extremely Stable Sodium Metal Batteries Enabled by Localized High-Concentration Electrolytes. *ACS Energy Lett.* **2018**, *3* (2), 315−321.
(99) Lu, Z.; Yang, H.; Yang, Q. H.; He, P.; Zhou, H. Building a Beyond Concentrated Electrolyte for High-Voltage Anode-Free Rechargeable Sodium Batteries. *Angew. Chem., Int. Ed.* **2022**, *61* (20), e202200410.
(100) Wu, E. A.; Banerjee, S.; Tang, H.; Richardson, P. M.; Doux, J. M.; Qi, J.; Zhu, Z.; Grenier, A.; Li, Y.; Zhao, E.; et al. A stable cathode-solid electrolyte composite for high-voltage, long-cycle-life solid-state sodium-ion batteries. *Nat. Commun.* **2021**, *12* (1), 1256.
(101) Deng, T.; Ji, X.; Zou, L.; Chiekezi, O.; Cao, L.; Fan, X.; Adebisi, T. R.; Chang, H. J.; Wang, H.; Li, B.; et al. Interfacial-engineering-enabled practical low-temperature sodium metal battery. *Nat. Nanotechnol* **2022**, *17* (3), 269−277.
(102) Hayashi, A.; Noi, K.; Sakuda, A.; Tatsumisago, M. Superionic glass-ceramic electrolytes for room-temperature rechargeable sodium batteries. *Nat. Commun.* **2012**, *3*, 856.
(103) Lazar, M.; Kmiec, S.; Joyce, A.; Martin, S. W. Investigations into Reactions between Sodium Metal and Na3PS4−xOx Solid-State Electrolytes: Enhanced Stability of the Na3PS3O Solid-State Electrolyte. *ACS Appl. Energy. Mater.* **2020**, *3* (12), 11559−11569.
(104) Su, Y.; Rong, X.; Gao, A.; Liu, Y.; Li, J.; Mao, M.; Qi, X.; Chai, G.; Zhang, Q.; Suo, L.; et al. Rational design of a topological polymeric solid electrolyte for high-performance all-solid-state alkali metal batteries. *Nat. Commun.* **2022**, *13*, 4181.
(105) Nanda, S.; Gupta, A.; Manthiram, A. Anode-Free Full Cells: A Pathway to High-Energy Density Lithium-Metal Batteries. *Adv. Energy Mater.* **2021**, *11* (2), 2000804.
(106) Tian, Y.; An, Y.; Wei, C.; Jiang, H.; Xiong, S.; Feng, J.; Qian, Y. Recently advances and perspectives of anode-free rechargeable batteries. *Nano Energy* **2020**, *78*, 105344.
(107) Ma, B.; Lee, Y.; Bai, P. Dynamic Interfacial Stability Confirmed by Microscopic Optical Operando Experiments Enables High-Retention-Rate Anode-Free Na Metal Full Cells. *Adv. Sci.* **2021**, *8* (12), 2005006.
(108) Wang, G.; Yu, M.; Feng, X. Carbon materials for ion-intercalation involved rechargeable battery technologies. *Chem. Soc. Rev.* **2021**, *50* (4), 2388−2443.
(109) Zhou, J.; Wang, Y.; Wang, J.; Liu, Y.; Li, Y.; Cheng, L.; Ding, Y.; Dong, S.; Zhu, Q.; Tang, M.; et al. Low-temperature and high-rate sodium metal batteries enabled by electrolyte chemistry. *Energy Stor. Mater.* **2022**, *50*, 47−54.
(110) Rudola, A.; Gajjela, S. R.; Balaya, P. High energy density in-situ sodium plated battery with current collector foil as anode. *Electrochem. Commun.* **2018**, *86*, 157−160.
(111) Li, Y.; Zhou, Q.; Weng, S.; Ding, F.; Qi, X.; Lu, J.; Li, Y.; Zhang, X.; Rong, X.; Lu, Y.; Wang, X.; Xiao, R.; Li, H.; Huang, X.; Chen, L.; Hu, Y.-S. Interfacial engineering to achieve an energy density of over 200 Wh kg^{-1} in sodium batteries. *Nat. Energy* **2022**, *7* (6), 511−519.
(112) Cohn, A. P.; Muralidharan, N.; Carter, R.; Share, K.; Pint, C. L. Anode-Free Sodium Battery through in Situ Plating of Sodium Metal. *Nano Lett.* **2017**, *17* (2), 1296−1301.
(113) Wang, L.; Ren, N.; Yao, Y.; Yang, H.; Jiang, W.; He, Z.; Jiang, Y.; Jiao, S.; Song, L.; Wu, X.; Wu, Z. S.; Yu, Y. Designing Solid Electrolyte Interfaces towards Homogeneous Na Deposition: Theoretical Guidelines for Electrolyte Additives and Superior High-Rate Cycling Stability. *Angew. Chem., Int. Ed.* **2023**, *62* (6), e202214372.
(114) Wang, Z.; Li, M.; Ruan, C.; Liu, C.; Zhang, C.; Xu, C.; Edström, K.; Strømme, M.; Nyholm, L. Conducting Polymer Paper-Derived Mesoporous 3D N-doped Carbon Current Collectors for Na and Li Metal Anodes: A Combined Experimental and Theoretical Study. *J. Phys. Chem. C* **2018**, *122* (41), 23352−23363.
(115) Liu, S.; Tang, S.; Zhang, X.; Wang, A.; Yang, Q. H.; Luo, J. Porous Al Current Collector for Dendrite-Free Na Metal Anodes. *Nano Lett.* **2017**, *17* (9), 5862−5868.
(116) Lee, K.; Lee, Y. J.; Lee, M. J.; Han, J.; Lim, J.; Ryu, K.; Yoon, H.; Kim, B. H.; Kim, B. J.; Lee, S. W. A 3D Hierarchical Host with Enhanced Sodiophilicity Enabling Anode-Free Sodium-Metal Batteries. *Adv. Mater.* **2022**, *34* (14), 2109767.
(117) Xu, J.; Xie, Y.; Zheng, J.; Liu, C.; Lai, Y.; Zhang, Z. A sodiophilic carbon cloth decorated with Bi-MOF derived porous Bi@C nanosheets for stable Na metal anode. *J. Electroanal. Chem.* **2021**, *903*, 115853.
(118) Tang, S.; Qiu, Z.; Wang, X.-Y.; Gu, Y.; Zhang, X. G.; Wang, W. W.; Yan, J. W.; Zheng, M. S.; Dong, Q. F.; Mao, B. W. A room-temperature sodium metal anode enabled by a sodiophilic layer. *Nano Energy* **2018**, *48*, 101−106.
(119) Cohn, A. P.; Metke, T.; Donohue, J.; Muralidharan, N.; Share, K.; Pint, C. L. Rethinking sodium-ion anodes as nucleation layers for anode-free batteries. *J. Mater. Chem. A* **2018**, *6* (46), 23875−23884.
(120) Chen, X.; Bai, Y. K.; Shen, X.; Peng, H. J.; Zhang, Q. Sodiophilicity/potassiophilicity chemistry in sodium/potassium metal anodes. *J. Energy Chem.* **2020**, *51*, 1−6.
(121) Hu, X.; Matios, E.; Zhang, Y.; Wang, C.; Luo, J.; Li, W. Enabling stable sodium metal cycling by sodiophilic interphase in a polymer electrolyte system. *J. Energy Chem.* **2021**, *63*, 305−311.
(122) Liu, P.; Yi, H.; Zheng, S.; Li, Z.; Zhu, K.; Sun, Z.; Jin, T.; Jiao, L. Regulating Deposition Behavior of Sodium Ions for Dendrite-Free Sodium-Metal Anode. *Adv. Energy Mater.* **2021**, *11* (36), 2101976.
(123) Suo, L.; Borodin, O.; Sun, W.; Fan, X.; Yang, C.; Wang, F.; Gao, T.; Ma, Z.; Schroeder, M.; von Cresce, A.; Russell, S. M.; Armand, M.; Angell, A.; Xu, K.; Wang, C. Advanced High-Voltage Aqueous Lithium-Ion Battery Enabled by "Water-in-Bisalt" Electrolyte. *Angew. Chem., Int. Ed. Engl.* **2016**, *55* (25), 7136−7141.

https://doi.org/10.1021/acscentsci.3c00301
ACS Cent. Sci. 2023, 9, 1076−1087